

RESEARCH PAPER

A dual band-notched ultra-wideband monopole antenna with spiral-slots and folded SIR-DGS as notch band structures

SEYED SAEED MIRMOSAEI¹, SEYED EBRAHIM AFJEI², ESFANDIAR MEHRSHAHI³
AND MOHAMMAD M. FAKHARIAN⁴

In this paper, an ultra-wideband (UWB) planar monopole antenna with impedance bandwidth from 2.83 to 11.56 GHz and dual band-notched characteristics is presented. The antenna consists of a small rectangular ground plane, a bat-shaped radiating patch, and a 50-Ω microstrip line. The notched bands are realized by introducing two different types of structures. The half-wavelength spiral-slots are etched on the radiating patch to obtain a notched band in 5.15–5.925 GHz for WLAN, HIPERLAN, and DSRC systems. Based on the single band-notched UWB antenna, the second notched band is realized by etching a folded stepped impedance resonator as defected ground structure on the ground plane for WiMAX and C-band communication systems. The notched frequencies can be adjusted by altering the length of resonant cells. Surface current distributions and equivalent circuit are used to illustrate the notched mechanism. The performance of this antenna both by simulation and by experiment indicates that the proposed antenna is suitable and a good candidate for UWB applications.

Keywords: Antennas and propagation for wireless systems, Antenna design, Modeling and measurements

Received 3 November 2014; Revised 19 March 2015; Accepted 22 March 2015; first published online 27 April 2015

I. INTRODUCTION

After the allocation of the frequency band from 3.1 to 10.6 GHz for the commercial use of ultra-wideband (UWB) systems by the Federal Communication Commission, UWB systems have received phenomenal gravitation in wireless communication. UWB radio technology has found application in medical imaging systems, pulse communication, ground penetration radar, and so on. Designing an antenna to operate in the UWB band is quite a challenge because it has to satisfy the requirements such as ultra wide impedance bandwidth, omnidirectional radiation pattern, constant gain, high radiation efficiency, low profile, easy manufacturing, and etc [1].

In UWB communication systems, one of the key issues is the design of a compact antenna while providing wideband characteristic over the whole operating band. Consequently, a number of UWB antennas with different geometries have been experimentally characterized [2–4]. Among them, planar monopole antennas are considered as good candidates for UWB applications due to their attractive merits, such as large impedance bandwidth, easy fabrication, and omnidirectional radiation pattern [5]. Especially in the case of microstrip

UWB planar monopole antenna, different methods have been utilized in the articles to design a UWB antenna with various band-notched properties [6–9]. Despite the advantages of UWB systems, there are many narrowband communication systems which severely interfere with the UWB communication system, such as worldwide interoperability for microwave access (WiMAX) (3.3–3.6 GHz), C-band (3.7–4.2 GHz), wireless local area network (WLAN) (5.15–5.35 GHz and 5.725–5.825 GHz), high performance radio LAN (HIPERLAN)/2 (5.47–5.725 GHz), and dedicated short-range communications (DSRC) (5.85–5.925 GHz). Therefore, UWB antennas with band-notched characteristics to filter this potential interference are desirable. The band-notched characteristics could be achieved by many techniques such as embedding of open-end slit to the antenna structure and addition of a tuning stub within the antenna structure or the ground plane [9], inserting different types of slots on the radiating patch or associated ground plane [10–12], addition of parasitic elements near the printed antennas [13], using different shapes of conductor-backed plane structures [14], locating filtering structures in the vicinity of the feed line [15], and so on. Among these methods, the primary methods are inserting $\lambda/2$ or $\lambda/4$ slots or stubs on the patch, feed-line or the ground plane. There are kinds of shapes for the slots and the stubs, such as U-shaped [7], H-shaped [8], C-shaped [16], L-shaped [17], π -shaped [18], and Ω -shaped [19]. Employing one structure sometimes can obtain multiple notched bands [8], or multiple notched band structure only introduce one resonance [20], which make it hard to analysis and adjust the notched band. On the other hand, in some

^{1,2,3}Department of Electrical and Computer Engineering, Shahid Beheshti University, Tehran, Iran

⁴Department of Electrical and Computer Engineering, Semnan Branch, Islamic Azad University, Semnan, Iran

Corresponding author:

M.M. Fakharian

Email: m_fakharian@semnaniau.ac.ir

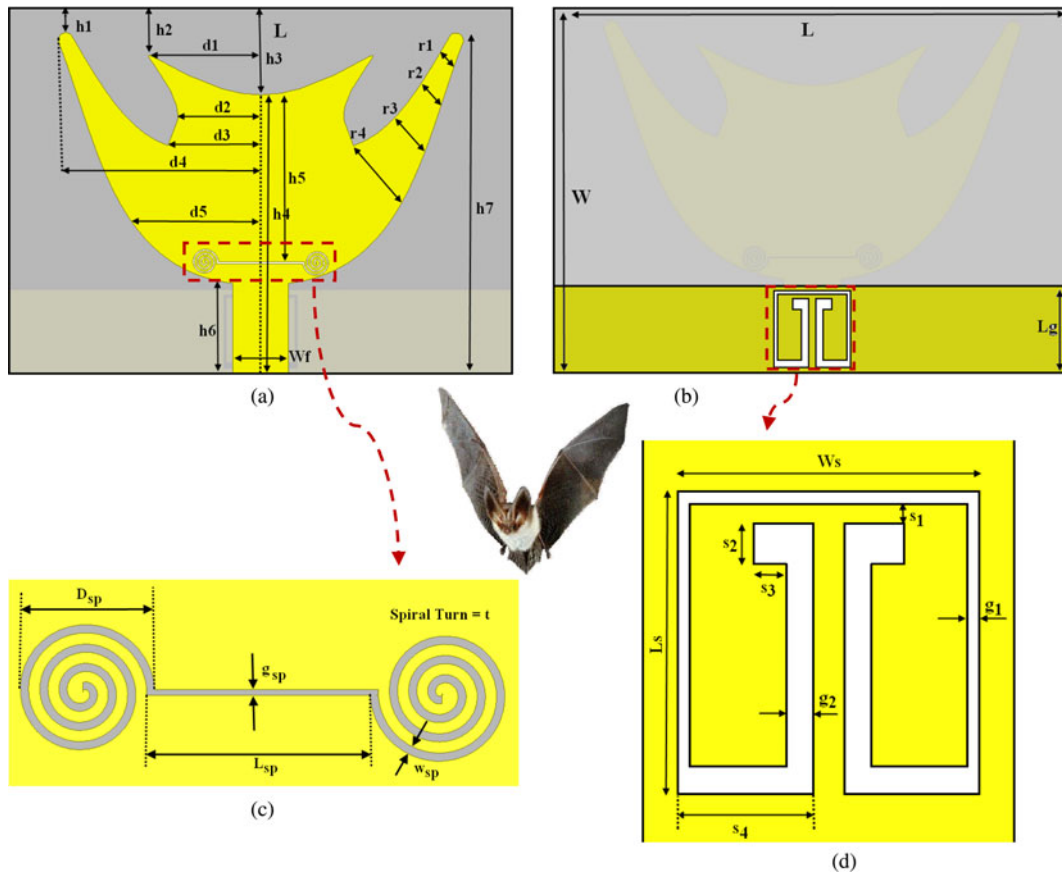


Fig. 1. Geometry of the proposed dual band-notch UWB antenna. (a) Top and (b) bottom view of the antenna, (c) parameters of spiral-slots and (d) SIR-DGS.

designs, the bandwidth of the notched bands is somewhat too wide so that useful signal is shielded at the same time [21, 22].

In this paper two methods for designing a novel and compact microstrip-fed monopole antenna with dual band-notched characteristic for UWB applications has been designed and manufactured. In the proposed structure a bat-shaped radiating patch is used to achieve a multi-resonance performance. By embedding the resonance elements, the proposed design can reject the frequency bands with central frequencies at 3.5 and 5.6 GHz without using an additional band-stop filter. By inserting the half-wavelength spiral-slots on the radiation patch, good band-notched performance with a high level of signal rejection can be achieved. While the other notched band is acquired by inserting folded stepped impedance resonator (SIR) as defected ground structure (DGS) on the ground plane of the antenna. These structures can resonant independently with tiny interference

among them. An equivalent circuit model of the proposed dual band-notched UWB antenna is extracted to explain the dual band-notched characteristics. Good reflection coefficient, radiation pattern, and group delay characteristics are obtained in the frequency band of interest. The simulated results are identical with the measured ones reasonably.

II. ANTENNA DESIGN AND CONFIGURATION

Figure 1 shows the geometry of the dual band-notched UWB bat-shaped monopole antenna fed by a 50-Ω microstrip line. The antenna is printed on a low-cost FR4 substrate of thickness 1.6 mm, permittivity 4.4, and loss tangent 0.02. The bat-shaped radiating element and feeding line are printed on the top side of the dielectric substrate and a rectangular ground

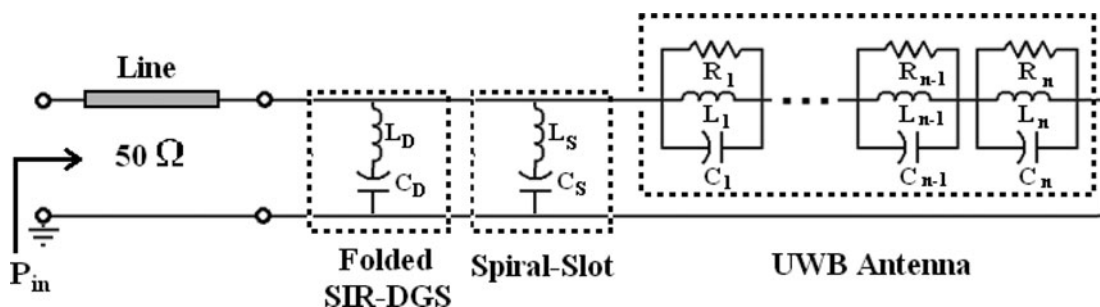


Fig. 2. Approximate equivalent circuit model for the proposed dual band-notch UWB antenna.

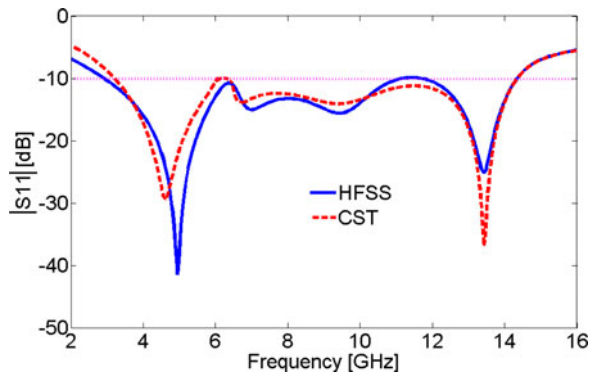





Fig. 3. Simulated $|S_{11}|$ of the proposed UWB antenna.

plane on the bottom side. In order to create single and dual band-filtering, spiral-slots and a SIR-DGS are inserted at radiating patch and ground plane, respectively. Figure 2 shows the approximate equivalent circuit model of the proposed dual band-notched UWB antenna [6, 23, 24].

The radiation patch has a bat-shaped structure, and the dimensions are improved using commercial software. The final design parameters of the UWB antenna are as follows: $L = 27$ mm, $W = 19$ mm, $L_g = 4.5$ mm, $W_f = 3$ mm, $h_1 = 0.7$ mm, $h_2 = 1.9$ mm, $h_3 = 4$ mm, $h_4 = 15$ mm, $h_5 = 9$ mm, $h_6 = 4.9$ mm, $h_7 = 18.4$ mm, $d_1 = 6$ mm, $d_2 = 4.5$ mm, $d_3 = 5$ mm, $d_4 = 10.8$ mm, $d_5 = 6.7$ mm, $r_1 = 0.7$ mm, $r_2 = 1.3$ mm, $r_3 = 2$ mm, $r_4 = 2.7$ mm.

Table 1. Three cases of UWB antenna with different values of bat-shaped radiating patch.

Case and design	h_1 (mm)	h_2 (mm)	d_4 (mm)
1. 	0.7	1.9	10.8
2. 	1.2	0.1	13
3. 	0.5	1.9	13

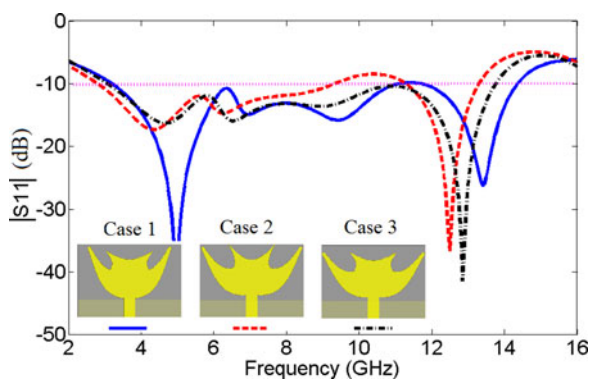


Fig. 4. The simulated $|S_{11}|$ characteristics for the three cases of UWB antenna with different values of bat-shaped radiating patch.



Fig. 5. Surface current around the spiral-slot of the proposed antenna at the notch frequency.

By examining the current distribution of planar monopole antenna with regular shapes, i.e. rectangular, circular, etc., the proposed cuttings in the bat-shaped monopole antenna are used to increase the antenna perimeter. It affects the lower resonant frequency and then increasing the maximum achieved impedance bandwidth [25, 26]. It is well known that the current distribution is mainly concentrated in the edges rather than in the center of the printed monopole antenna. Thus, by increasing the antenna perimeter p , the surface current will take longer path and this will be equivalent to a

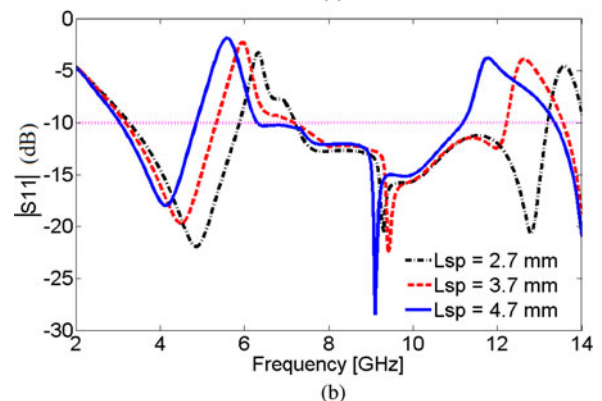
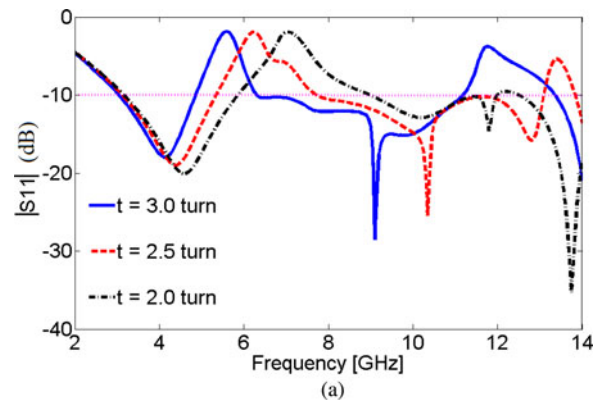


Fig. 6. Variation of reflection coefficient in terms of (a) t and (b) L_{sp} .

longer length monopole and in turn will decrease the lowest resonance frequency f_L [27]:

$$\epsilon_{eff} \approx \frac{(\epsilon_r + 1)}{2}, \tag{1}$$

$$f_L(\text{GHz}) = \frac{300}{p\sqrt{\epsilon_{eff}}}, \tag{2}$$

where ϵ_{eff} is the approximated effective dielectric constant and the perimeter unit is in millimeters.

For UWB antenna, the radiating element can be modeled by several adjacent resonances and each one can be represented by an *RLC* parallel circuit [16]. Approximately, the radiating element of the proposed UWB antenna can be seen as several parallel *RLC* cells in series, as shown in Fig. 2. Figure 3 shows the characteristics of the simulated reflection coefficient ($|S_{11}|$) of the UWB antenna by using Ansoft HFSS and CST Microwave Studio. A relative good agreement in between simulations can be observed. It is found that the $|S_{11}|$ of the antenna is well matched as the bandwidth covers the entire UWB frequency range

3.1–10.6 GHz and goes beyond the required 10.6 GHz with $|S_{11}| \leq -10$ dB.

To design a novel UWB monopole antenna, a bat-shaped radiating patch is used as initial structure in the proposed antenna, as displayed in Fig. 1(a). Three bat-shaped patch with different sizes are specified in Table 1 as cases 1–3. Figure 4 shows the effects of it with different values on the impedance matching. It is found that by setting the bat-shaped patch to suitable dimensions, the wider impedance bandwidth with multi-resonance characteristics can be produced, especially at the lower and higher bands.

A) Spiral-slots as notch band structure

In order to eliminate interferences from WLAN, HIPERLAN/2, and DSRC systems with the UWB, spiral-slots are etched on the radiating patch as a band rejection structure to cover the interval 5.15–5.925 GHz. As shown in Fig. 1(c), the spiral-slots are obtained by etching two separated spiral patterns which have same size and inverse split direction in the radiating patch. They are connected together by a rectangular-slot. The relationship between the notched frequency and the total length of spiral-slots can be summarized as following

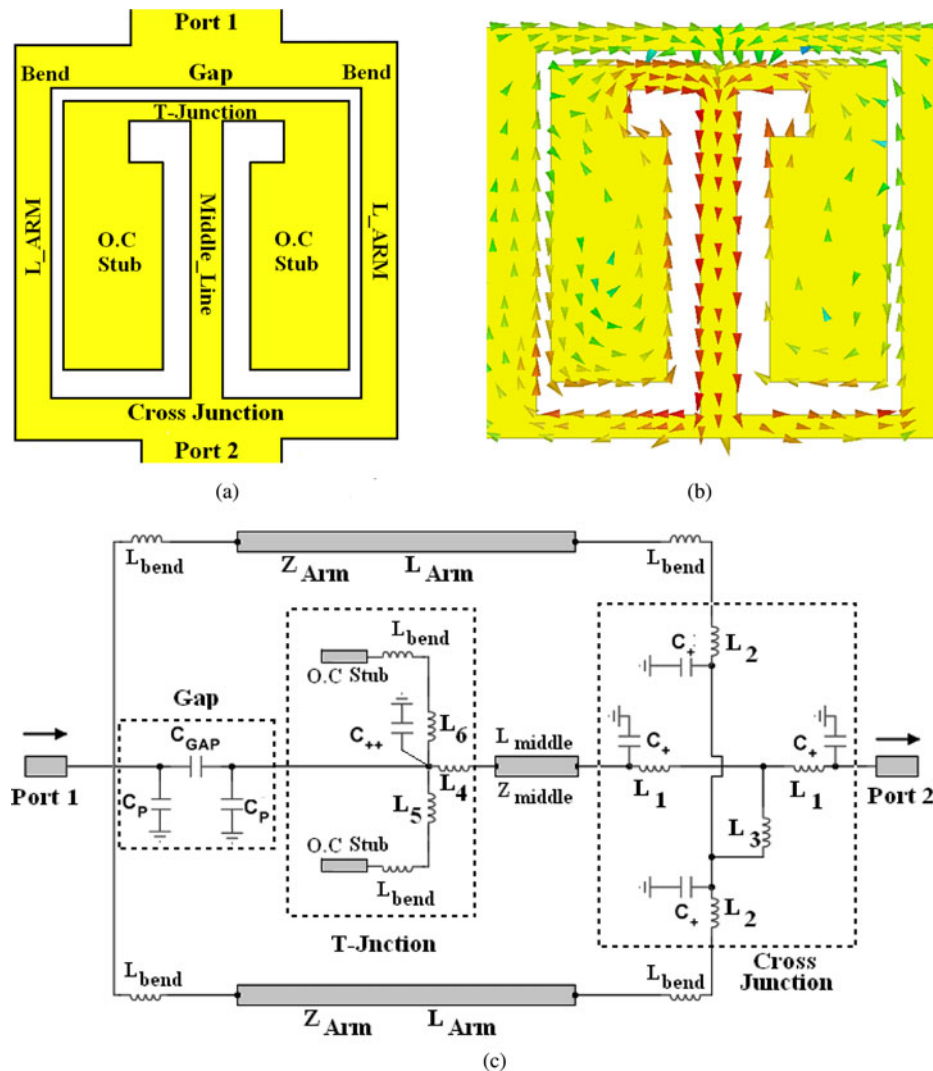


Fig. 7. (a) Equivalent filament model and (b) surface current of truncated structure of folded SIR-DGS on ground plane. (c) Quasi-static equivalent circuit model.

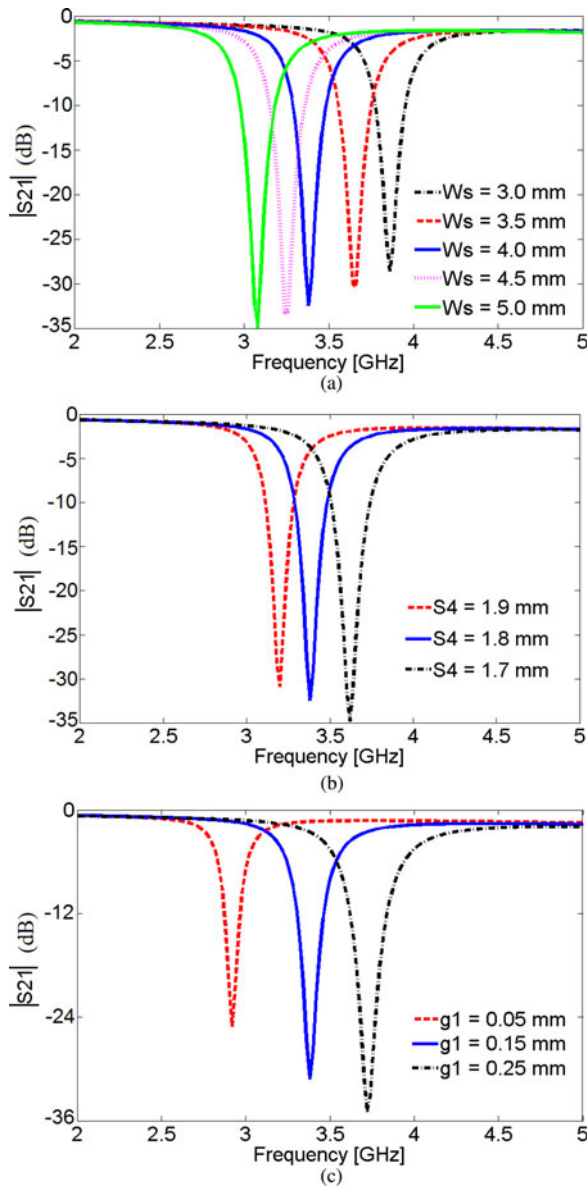


Fig. 8. Transfer characteristics of the SIR-DGS for various dimensions, (a) W_s , (b) S_4 , and (c) g_1 .

equations,

$$L_{cir} = \left[\left(\sum_{i=1}^t i \right) \times 2\pi W_{sp} \right] - t \times W_{sp}, \tag{3}$$

$$L = 2L_{cir} + L_{sp} - W_{sp} f_{notch} = \frac{c}{2L \times \sqrt{\epsilon_{eff}}},$$

where c is the speed of light in free space, t is the spiral turn, L_{cir} is the length of the spiral-slot, and L presents the total length of the slot. We can take (2) into account in obtaining the total length of the spiral-slots at the very beginning of the design and then adjust the geometry for the final design. At the notch frequency, current concentrates around the spiral-slots. In Fig. 5, since the antenna operates in a transmission-line-like mode [16], the impedance is very high (open circuit) at the middle of rectangular-slot and the impedance is nearly zero (short circuit) at the center of spiral-slots. The zero impedance at the feeding point leads

to the desired impedance mismatching at the notch frequency. Therefore, the spiral-slots can be modeled as a half-wavelength shorted parallel stub to act as the shunt series LC resonant for the band pass filter, as shown in Fig. 2. L_s and C_s indicate the inductor and capacitor values of the slot resonator. When the current propagates along the edge of the slot, an inductance should be introduced to the model. The narrow slot is equivalent to a capacitor. Increasing the length of the slot or decreasing the slot width is similar to increasing the capacitor value in the parallel LC circuit. On the other hand, increasing the length of slot will also lead to the increase of the inductor value [23]. It is found that by adjusting the total length of the spiral-slots to be approximately half-wavelength of the desired notched frequency, a destructive interference can take place, causing the antenna nonresponsive at that frequency. The final dimensions of the spiral-slots are as follows: $L_{sp} = 4.6$ mm, $W_{sp} = 0.1$ mm, $g_{sp} = 0.06$ mm, $D_{sp} = 1.4$ mm, and $t = 3.5$ turn.

It is easy to tune the notch center frequency with the change in total length of the slot. The effects of two different parameters t and L_{sp} of the slot on the band rejection performance of the presented design are also studied and shown in Fig. 6, where t is the spiral turn and L_{sp} is the length of the rectangular-slot. As observed in Fig. 6(a) that, the notched frequency is shifted from 5.6 to 7 GHz when t decreases from 3 to 2. Moreover, the increase in the bandwidth of the notched band can be observed with this change. Therefore, a wide notched band is obtained over the UWB frequency band when t is 2. It is also found that the performance of the reflection coefficient near 12 GHz becomes poor when t is 3. Taking the consideration of the performance and limited space for inserting the band-rejected elements, 3 is chosen for t in the design. In Fig. 6(b), when L_{sp} changes from 2.7 to 4.7 mm, the center frequency of the notched band moved from 6.3 to 5.6 GHz. These indicate that the center frequency of the notched band decreases as the length of the rectangular-slot increases. Interestingly, it is also found that the bandwidth of the reflection coefficient becomes wider when L_{sp} is shorter. It should be highlighted that, the value more than 4.7 mm is not considered to avoid the fabrication error. Since the notched band can cover 5–6 GHz when L_{sp} is equal to 4.7 mm, the length of the rectangular-slot is selected to be 4.7 mm.

B) Folded SIR-DGS as notch band structure

Besides WLAN, HIPERLAN/2, and DSRC systems, WiMAX and C-band may cause interferences to the UWB system too. By etching a folded SIR-DGS as band-notched structure on the ground plane, a band-notched function can be realized to cover the interval 3.3–4.2 GHz. As shown in Fig. 1(d), the folded SIR-DGS consists of low–high–low impedance slots, and the slots are etched on the ground plane. From the equivalent circuit model of Fig. 2, by inserting folded SIR defective pattern in the ground plane a parallel LC resonant circuit is added to the equivalent circuit. From the resonance condition $Z_{in} = 0$, the resonant frequency of a half-wavelength resonator can be deduced as follows,

$$L = 4L_s + W_s + 2S_4 + 2S_3 - 2S_1 - 2g_1, \tag{4}$$

$$f_{notch} = \frac{c}{2L \times \sqrt{\epsilon_{eff}}}$$

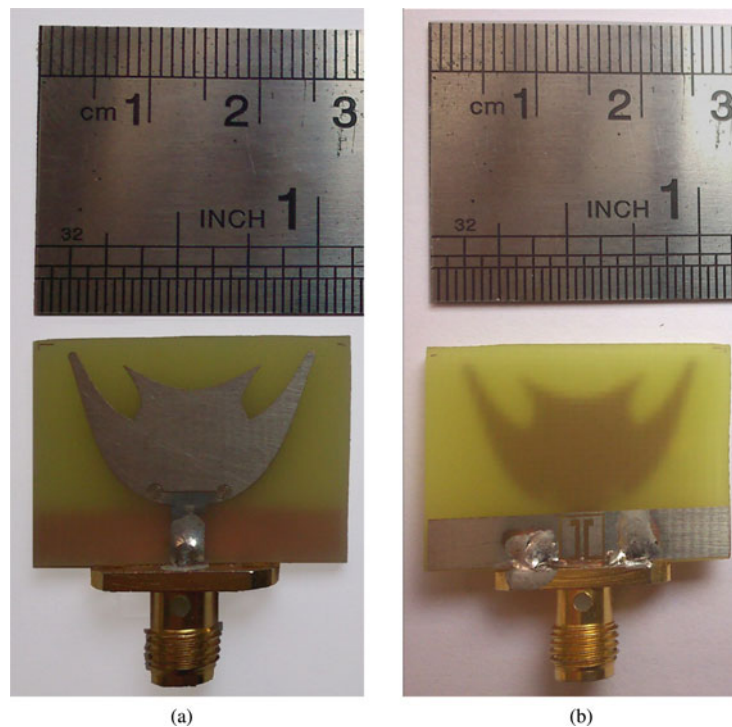


Fig. 9. Photograph of the realized printed monopole antenna, (a) top view, and (b) bottom view.

where L is the total length of the folded SIR-DGS. The improved parameters of the folded SIR-DGS are as follows: $W_s = 4$ mm, $L_s = 4$ mm, $g_1 = 0.16$ mm, $g_2 = 0.36$ mm, $S_1 = 0.27$ mm, $S_2 = 0.52$ mm, $S_3 = 0.44$ mm, and $S_4 = 1.8$ mm.

In order to better analyze the effect of these parameters, a quasi-static equivalent circuit model of the folded SIR-DGS is given in Fig. 7. The quasi-static equivalent circuit model is directly derived from the physical dimensions of DGS [28]. Figure 7(a) shows the equivalent filament model of the folded SIR-DGS. The current distribution of this compact model is shown in Fig. 7(b). As can be seen in this figure of the folded SIR-DGS perturbed microstrip transmission line, the return path of the current is fully disturbed and this current is confined to the periphery of the perturbation and returns below the microstrip line once the perturbation is over. Based on the observation of the maximum concentration of the return current, the width of the side filament arms,

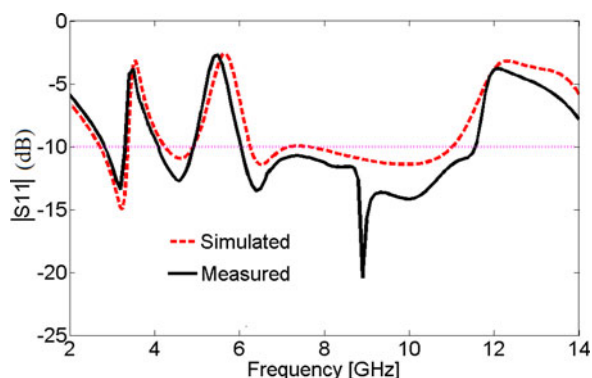


Fig. 10. Measured and simulated $|S_{11}|$ characteristics of the antenna.

which contribute to the inductance of the folded SIR-DGS, is selected.

Figure 7(c) shows the equivalent-circuit model of the folded SIR-DGS. Taking into consideration the aforementioned closed-form expressions and circuit parameters, we model the equivalent circuit of the truncated figure and then carry on the following conversions using the two-port circuit parameters. The width of the ports considered here corresponds to $50\text{-}\Omega$ characteristic impedance. The gap is represented by the equivalent capacitances and is connected vertically to the arms of the two crosses. The power is impinged at one arm of the cross and power is extracted from the opposite arm of another cross. Now the equivalent-circuit model of the current filament can be extracted with the equivalent inductances and capacitances of the microstrip discontinuities. The inductances and capacitances are derived from the physical dimensions using quasi-static expressions for microstrip crosses, bent lines, and gaps capacitances are fully characterized by 17 equations in the literature [28]. All these expressions take care of the dimensions of the DGS and the dielectric properties of the substrate. Therefore, from the equivalent-circuit model, a direct correlation between the design parameters and the design specification is calculated. The gaps are represented by two parallel capacitances to ground (C_P) and a series capacitance (C_{GAP}). The values of these capacitances are extracted from even- and odd-mode capacitances. Interestingly, it should be noted that all equivalent capacitances are extracted from the physical dimensions of the gap discontinuity and the dielectric constant [29]. If two conductors meet at an angle, mutual inductance comes to play at the bend, which we represented as L_{bend} in the circuit diagram (Fig. 7(c)). Two sets of two symmetrical arms of the microstrip cross are represented by equivalent L_1 , L_2 , C_+ , and the cross arms are inductively coupled by L_3 . The

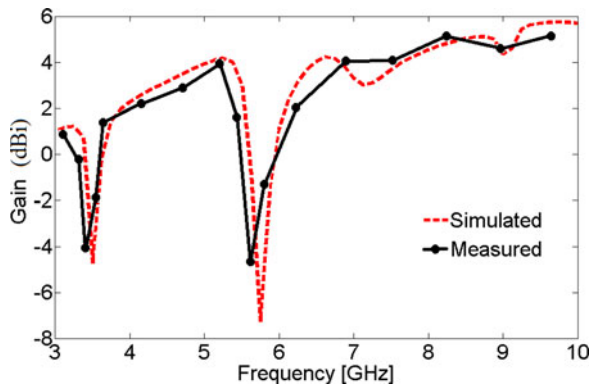


Fig. 11. Measured and simulated gains of the antenna.

equivalent capacitances and inductances are calculated in the literature [29].

To compare the frequency response characteristics of the folded SIR-DGS, a two-port filter structure consisting of a combination of a resonator and a 50-microstrip line is simulated. The structure is printed on the substrate with a permittivity of 4.4 and a thickness of 1.6 mm. The transfer characteristics of the folded SIR-DGS with various dimensions are shown in Fig. 8. It can be seen that the notched band decreases as W_s and S_4 increase. But the notched band increases as g_1 increases. Also by changing the g_1 of the folded SIR-DGS, we can change the width of the notched band. Therefore the notched band can be obtained at the desired frequency by appropriately adjusting the resonator dimensions. Moreover, by the electrical model in Fig. 7, a physical insight into the behavior of the antenna is given for the parametric analysis in Fig. 8. The variation of the resonant frequencies of the folded SIR-DGS with the arm length W_s and S_4 are due to the fact that when these parameters increase the inductance from the folded SIR-DGS increases, hence, the resonant frequency of the parallel circuit decreases. The variation of the resonant frequency with the gap distance g_1 is due to the fact that when the gap distance increases, the gap capacitance diminishes. As a result, the resonant frequency increases with the increase of the gap distance.

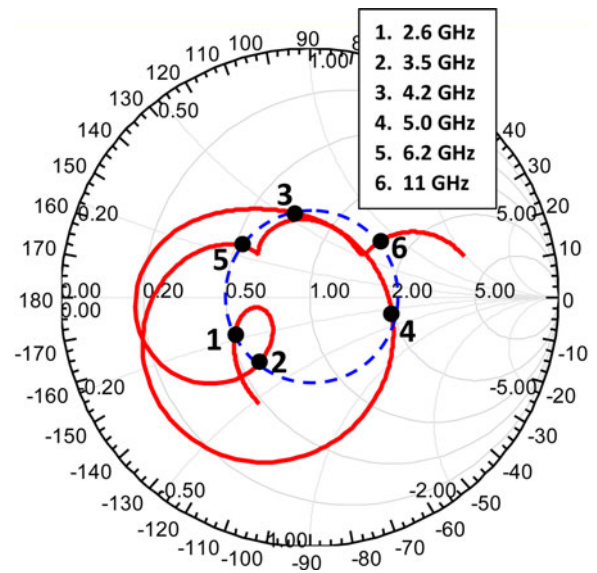


Fig. 12. Input impedance performance of the proposed antenna.

III. RESULTS AND DISCUSSION

The proposed dual band-notched UWB antenna with final modified design parameters, as shown in Fig. 9, was built and tested. Figure 10 shows the simulated and measured $|S_{11}|$ characteristics of the antenna. Simulation is carried out using Ansoft HFSS, a commercial three-dimensional (3D) electromagnetic simulator based on finite element method. The fabricated antenna has the frequency band of 2.83 to 11.56 GHz with two rejection bands around 3.3–4.2 and 4.9–6 GHz. The simulated gain and the measured one decrease over these two band-notched frequencies, as shown in Fig. 11. However, as shown in Figs 10 and 11, there exists a discrepancy between the measured data and the simulated results. This discrepancy is mostly due to a number of parameters such as fabrication inaccuracies (e.g. over-etching), uncertainties in the substrate thickness and effective permittivity, the wide range of simulation frequencies, and so on. However since substrate materials may vary among manufacturers, the design methodology, and proof of concept are the main foci of this work. In order to confirm the accurate

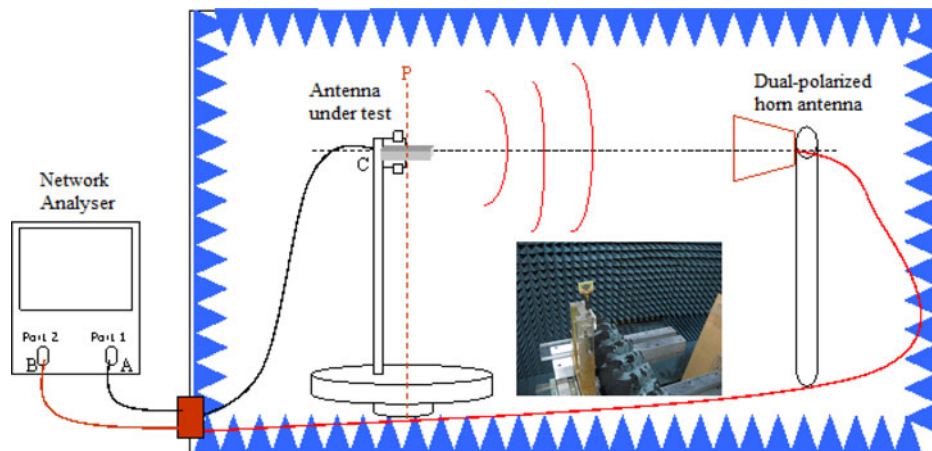


Fig. 13. Measurement set-up of the antenna for radiation patterns.

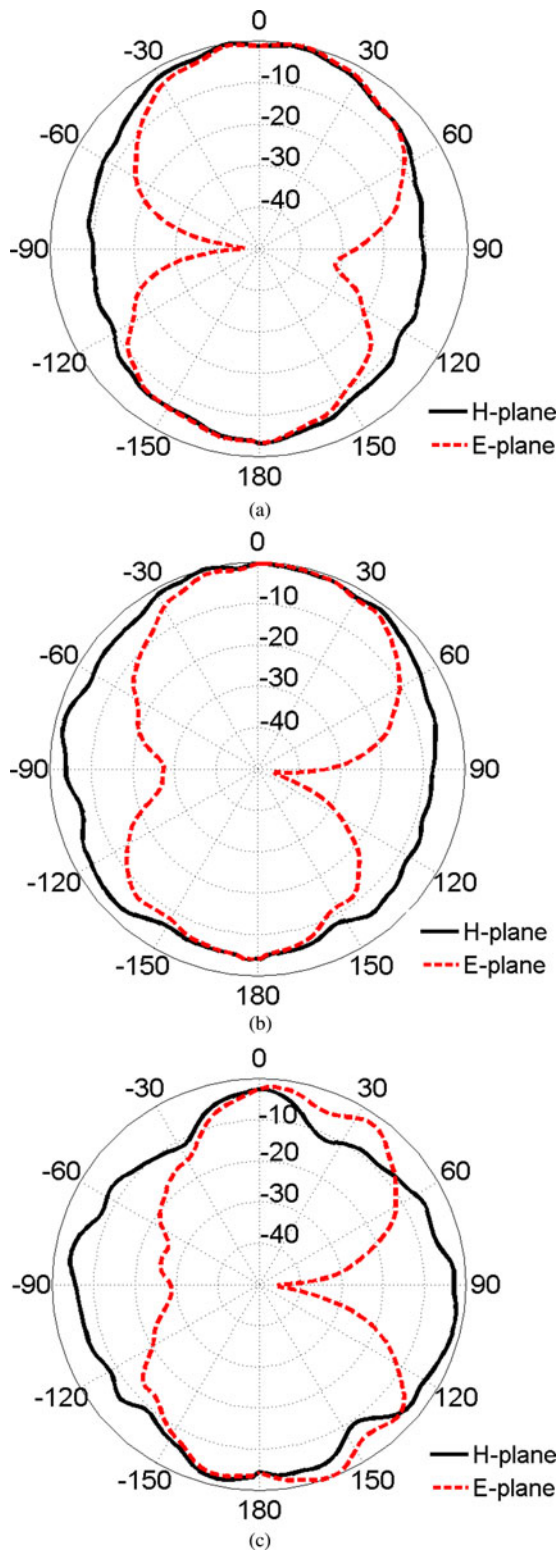


Fig. 14. Measured radiation patterns of the proposed antenna in the E- and H-planes at (a) 3 GHz, (b) 6.5 GHz, and (c) 10 GHz.

reflection coefficient characteristics for the designed antenna, it is recommended that the manufacturing and measurement processes need to be performed carefully. Moreover, SubMiniature version A (SMA) soldering accuracy and FR4 substrate quality need to be taken into consideration.

To give a better insight about the dual band-notch behavior of the proposed antenna, a simulated input impedance

characteristic at the band-notch performance is shown on a Smith chart in Fig. 12.

Measurement set-up of the antenna for the radiation pattern characteristics is shown in Fig. 13. Figure 14 depicts the measured far-field radiation patterns for the proposed dual-band notched UWB antenna in the E-(xy-) and H-(xz-) planes at 3, 6.5 and 10 GHz. It is observed that nearly omnidirectional radiation patterns are obtained on H-plane over the whole UWB frequency range. The radiation patterns on the E-plane are monopole-like with bidirectional patterns in a very wide frequency band. It is observed that the radiation pattern is slightly tilted off-broadside. The beam tilt is due to the asymmetrical geometry of the patch antenna, compared with a simply patch which has a symmetrical geometry and shows a broadside beam. As the frequency goes up, tiny distortions occur. This is because the electrical length of the antenna increases at higher frequency.

To analyze the signal dispersion, the group delay is simulated between two identical antennas in the face-to-face orientations, with a distance of 300 mm between them, which obtains the far-field condition of the antenna. As shown in Fig. 15, the group delay is about 1 ns across the frequency band except in the notched bands, due to the band-notched function. For the rest of the frequency band, the group delay characteristic is relatively flat, indicating that the antennas have good linear transmission performances.

As the UWB communication has been based on impulse radio, it is necessary to consider the impulse distortion of the time-domain response of the proposed antenna. In telecommunication systems, the correlation between the input and output signals is evaluated using the fidelity factor F (1),

$$F = \max_{\tau} \left| \frac{\int_{-\infty}^{+\infty} s(t)r(t - \tau) dt}{\sqrt{\int_{-\infty}^{+\infty} s(t)^2 dt \cdot \int_{-\infty}^{+\infty} r(t)^2 dt}} \right|, \quad (5)$$

where $s(t)$ and $r(t)$ are the input and output signals, respectively. To calculate the fidelity factor of the proposed dual-band notched UWB antenna, it is assumed that the two proposed antennas in Fig. 1 play the role of the transmitting antenna and receiving antenna. The two antennas are aligned pointing face-to-face and side-by-side orientations with a distance of 300 mm. The input signal $s(t)$ form of the Gaussian pulse

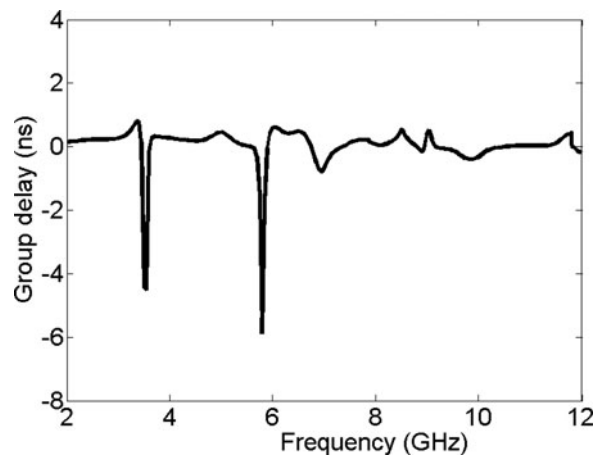


Fig. 15. Simulated group delay of the proposed antenna.

can be excited to transmitting antenna, then receiving pulse signal $r(t)$ can be obtained to receiving antenna. This pulse simulation is performed by a CST Design Studio simulator. By substituting the two normalized pulse signal in equation (5), we can calculate the fidelity factor F which is the maximum correlation coefficient between two pulse signals. The antenna having $F=1$ indicates a perfect match between $s(t)$ and $r(t)$, without distortion in the transmission system of the pulse signal. The fidelity factor F of the proposed dual-band notched UWB antenna for the face-to-face and side-by-side configurations were obtained equal to 0.92 and 0.86, respectively. Values of the fidelity factor show that the proposed UWB antenna exhibits a good time domain performance in the view of operating UWB communication systems.

IV. CONCLUSION

A dual band-notched UWB antenna has been proposed and designed by introducing the folded SIR-DGS and the spiral-slots as band-rejected elements. In this design, the proposed antenna can operate from 2.83 to 11.56 with two rejection bands around 3.3–4.2 and 4.9–6 GHz. Parametric studies, relevant equations and the equivalent circuit model of the antenna provide guidelines on how to understand the mechanism of band-notched characteristics. Good agreement between the simulated and measured results including stable radiation patterns, gain, and low $|S_{11}|$ (except for the notched bands) for all radiating frequencies is obtained. It demonstrates that the proposed antenna is suitable for application in UWB system.

REFERENCES

- [1] Fakharian, M.M.; Rezaei, P.: Very compact palmate leaf-shaped CPW-FED monopole antenna for UWB applications. *Microw. Opt. Technol. Lett.*, **56** (2014), 1612–1616.
- [2] Wang, J.H.; Yin, Y.Z.; Liu, X.L.; Wang, T.: Trapezoid UWB antenna with dual band-notched characteristics for WiMAX/WLAN bands. *Electron. Lett.*, **49** (2013), 685–686.
- [3] Bod, M.; Hassani, H.R.; Samadi Taheri, M.M.: Compact UWB printed slot antenna with extra bluetooth, GSM, and GPS bands. *IEEE Antennas Wireless Propag. Lett.*, **11** (2012), 531–534.
- [4] Fakharian, M.M.; Rezaei, P.; Azadi, A.: A planar UWB bat-shaped monopole antenna with dual band-notched for WiMAX/WLAN/DSRC. *Wireless Pers. Commun.*, **81** (2015), 881–891.
- [5] Foudazi, A.; Hassani, H.R.; Nezhad, S.M.A.: Small UWB planar monopole antenna with added GPS/GSM/WLAN bands. *IEEE Trans. Antennas Propag.*, **60** (2012), 2987–2992.
- [6] Abed, D.; Kimouche, H.: Design and characterization of microstrip UWB antennas, ultrawideband, in Lembrikov, B. (ed.), *InTech, Scio, Croatia* (2010), ISBN: 978-953-307-139-82.
- [7] Lee, W.S.; Lim, W.G.; Yu, J.W.: Multiple band-notched planar monopole antenna for multiband wireless systems. *IEEE Microw. Wireless Compon. Lett.*, **15** (2005), 576–578.
- [8] Sung, Y.: Triple band-notched UWB planar monopole antenna using a modified H-shaped resonator. *IEEE Trans. Antennas Propag.*, **61** (2013), 953–957.
- [9] Sarkar, P.; Rakshit, I.; Adhikari, S.; Pal, M.; Ghatak, R.: A band notch UWB bandpass filter using dual-stub-loaded multimode resonator with embedded spiral resonator. *Int. J. Microw. Wireless Technol.*, **6** (2014), 161–166.
- [10] Li, W.T.; Hei, Y.Q.; Feng, W.; Shi, X.W.: Planar antenna for 3G/Bluetooth/WiMAX and UWB applications with dual band-notched characteristics. *IEEE Antennas Wireless Propag. Lett.*, **11** (2012), 61–64.
- [11] Sharbati, V.; Rezaei, P.; Shahzadi, A.; Fakharian, M.M.: A planar UWB antenna based on MB-OFDM applications with switchable dual band-notched for cognitive radio systems. *Int. J. Microw. Wireless Technol.*, available on CJO2014, doi:10.1017/S1759078714001317. <http://journals.cambridge.org/action/displayAbstract?fromPage=online&aid=9384424>
- [12] Azim, R.; Islam, M.T.: Compact planar UWB Antenna with band notch characteristics for WLAN and DSRC. *Prog. Electrom. Res.*, **133** (2013), 391–406.
- [13] Jiang, W.; Che, W.: A novel UWB antenna with dual notched bands for WiMAX and WLAN applications. *IEEE Antennas Wireless Propag. Lett.*, **11** (2012), 293–296.
- [14] Ojaroudi, M.; Ojaroudi, N.; Mirhashemi, S.A.: Bandwidth enhancement of small square monopole antenna with dual band-notch characteristics by using an H-ring slot and conductor backed plane for UWB applications. *Appl. Comput. Electrom. Soc. J.*, **28** (2013), 64–70.
- [15] Sung, Y.: UWB monopole antenna with two notched bands based on the folded stepped impedance resonator. *IEEE Antennas Wireless Propag. Lett.*, **11** (2012), 500–502.
- [16] Chu, Q.-X.; Yang, Y.-Y.: A compact ultrawideband antenna with 3.4/5.5 GHz dual band-notched characteristics. *IEEE Trans. Antennas Propag.*, **56** (2008), 3637–3644.
- [17] Farrokh-Heshmat, N.; Nourinia, J.; Ghobadi, Ch.: Band-notched ultra-wideband printed open-slot antenna using variable on-ground slits. *Electron. Lett.*, **45** (2009), 1060–1061.
- [18] Valzade, A.; Ghobadi, Ch.; Nourinia, J.; Ojaroudi, M.: A novel design of reconfigurable slot antenna with switchable band notch and multiresonance functions for UWB applications. *IEEE Antennas Wireless Propag. Lett.*, **11** (2012), 1166–1169.
- [19] Li, W.T.; Shi, X.W.; Hei, Y.Q.: Novel planar UWB monopole antenna with triple band-notched characteristics. *IEEE Antennas Wireless Propag. Lett.*, **8** (2009), 1094–1098.
- [20] Zheng, Z.-A.; Chu, Q.-X.; Tu, Z.-H.: Compact band-rejected ultrawideband slot antennas inserting with $\lambda/2$ and $\lambda/4$ resonators. *IEEE Trans. Antennas Propag.*, **59** (2011), 390–397.
- [21] Lee, D.-H.; Yang, H.-Y.; Cho, Y.-K.: Tapered slot antenna with band-notched function for ultrawideband radios. *IEEE Antennas Wireless Propag. Lett.*, **11** (2012), 682–685.
- [22] Zhu, F.; Gao, S.; Ho, A.T.S.; Abd-Alhameed, R.A.; See, C.H.; Li, J.; Xu, J.: Miniaturized tapered slot antenna with signal rejection in 5–6-ghz band using a balun. *IEEE Antennas Wireless Propag. Lett.*, **11** (2012), 507–510.
- [23] Yu, F.; Wang, C.: Design of a CPW-fed dual band-notched planar wideband antenna for UWB applications, ultrawideband communications: novel trends – antennas and propagation, in Dr. Matin, M. (ed.), *InTech, Rijeka, Croatia* (2011), ISBN: 978-953-307-452-8.
- [24] Wei, F.; Xu, L.; Shi, X.-W.; Liu, B.: Compact UWB bandpass filter with two notch bands based on folded SIR. *Electron. Lett.*, **46** (2010), 1679–1680.
- [25] Ahmed, O.M.H.; Sebak, A.R.: A novel maple-leaf shaped UWB antenna with a 5.0–6.0 GHz band-notch characteristic. *Prog. Electron. Res. C*, **11** (2009), 39–49.

- [26] Azenui, N.C.; Yang, H.Y.D.: A printed crescent patch antenna for ultrawideband applications. *IEEE Antennas Wireless Propag. Lett.*, **6** (2007), 113–116.
- [27] Ahmed, O.; Sebak, A.: A printed monopole antenna with two steps and a circular slot for UWB applications. *IEEE Antennas Wireless Propag. Lett.*, **7** (2008), 411–413.
- [28] Karmakar, N.C.; Roy, S.M.; Balbin, I.: Quasi-static modeling of defected ground structure. *IEEE Trans. Microw. Theory Tech.*, **54** (2006), 2160–2168.
- [29] Garg, R.; Bahl, I.J.: Microstrip discontinuities. *Int. J. Electron.*, **45** (1978), 81–87.



Seyed Saeed Mirmosaei was born in Ramsar, Iran, in 1986. He received his B.S. degree in Electrical Engineering from Guilan University, Rasht, Iran, in 2008. Currently, he is working towards the M.Sc. degree in Communication Engineering from Shahid Beheshti University, Tehran, Iran. His research interests include ultra-wideband monopole antennas.



Seyed Ebrahim Afjei received his B.S. and M.S. degrees in Electrical Engineering from the University of Texas in 1984, 1986, respectively, and the Ph.D. degree from New Mexico State University, in 1991. He is currently a Professor and Dean of the Department of Electrical Engineering, Shahid Beheshti University G.C., Tehran, IRAN. His research

interests are in the areas of switched reluctance motor drives, numerical analysis, and power electronics.



Esfandiar Mehrshahi was born in Tehran, Iran, in 1963. He received his B.Sc. degree from the Iran University of Science and Technology, Tehran, Iran, in 1987, and the M.Sc. and Ph.D. degrees from the Sharif University of Technology, Tehran, Iran, in 1991 and 1998, respectively, all in Electrical Engineering. Since 1990, he has been involved in several research and engineering projects at the Iran Telecommunications Research Center (ITRC). He is currently an Assistant Professor at Shahid Beheshti University, Tehran, Iran. His main areas of interest are the nonlinear simulation of microwave circuits, computational electromagnetics, and low phase noise oscillators.



Mohammad M. Fakharian was born in Tehran, Iran, in 1987. He received his B.S. and M.S. degrees in Electrical Engineering from Semnan University, Semnan, Iran, in 2009 and 2012, respectively. Currently, he is working towards the Ph.D. degree in Communication Engineering from Semnan University. His research interests include

low-profile printed and patch antennas for wireless communication, fractal, miniature and multiband antennas, metamaterials and EBG structures interaction with antennas and RF passive components, reconfigurable antennas, and electromagnetic theory: numerical methods and optimization techniques.